Study of chemical field effect transistors for the detection of ammonium and nitrate ions in liquid and soil phases

Matthieu Joly, M. Marlet, C. Durieu, Camille Bene, Jérôme Launay, Pierre Temple-Boyer

STUDY OF CHEMICAL FIELD EFFECT TRANSISTORS FOR THE DETECTION OF AMMONIUM AND NITRATE IONS IN LIQUID AND SOIL PHASES

M. Joly[1,2,3], M. Marlet[3], C. Durieu[3], C. Bene[1,2], J. Launay[1,2], P. Temple-Boyer[1,2]

1) CNRS, LAAS, 7 avenue du colonel Roche, F-31400 Toulouse, France

2) University of Toulouse; INSAT, UPS; LAAS; F-31400 Toulouse, France

3) Agronutrition SA, F-31390 Carbonne, France

Abstract: the development of ChemFET-based sensors for the soil analysis of nitrogen-based ions is described in this work. Focusing on the fluoropolysiloxane (FPSX) polymer-based matrix, nonactin and tetradodecylammonium nitrate (TDDAN) were shown to have the best properties for the detection of ammonium NH_4^+ and nitrate NO_3^- ions respectively. Thus, FPSX-based pNH_4-ISFET and pNO_3-ISFET microsensors exhibited good detection properties (sensitivity around 56 mV/pX in concentration ranges adapted to soil analysis) and acceptable selectivity to soil main interferent ions (K^+, Na^+, Ca^{2+}, Cl^-, $H_2PO_4^{2-}$, SO_4^{2-},…). Following, the two different ISFET sensors were applied to the in-situ soil analysis. Thus, using standard relative moistures, pH analysis in clay-silt matrixes was demonstrated on a six-month period (compatible with agriculture applications during the fertilization period). Then, experimental studies were successfully extended to the monitoring of nitrogen mineralization through pNH_4 measurement, as well as to the analysis of soil nitration processes. Finally, long-term analyses were performed, showing contradictory result according to the chosen ionophore: a "zero" temporal drift on a six-month period for nonactin and PFSX-based pNH_4-ISFET, and a huge temporal drift for TDDAN and PFSX-based pNO_3-ones. This work paves the way for future long-term ionic analyses in soil matrix.

Keywords: ion-sensitive field effect transistor, potentiometric sensor, ion-sensitive layers, ammonium NH_4^+ ion, nitrate NO_3^- ion, soil analysis

1. Introduction

The nitrogen element, symbol N, is essential for the growth and development of plants. It represents between 1% and 5% of their dry matter [1] and plays an important role for the synthesis of their amino-acids, proteins, enzymes and chlorophyll-related molecules [2]. However, despite the abundance of diazote N_2 in the atmosphere (volume ratio: 78%), the sources of nitrogen for plants are mainly limited to the "N element" main mineral forms: the ammonium NH_4^+ and nitrate NO_3^- ions, present in soils at different concentration ranges, i.e. 20 – 200 µM and 1 – 5 mM respectively [3]. Because of their greater mobility, nitrate ions are more easily absorbed by roots than ammonium ions, which are partly retained in the soil matrix. Nevertheless, both ionic species, as well as their derivative chemicals, are largely involved into the nitrogen cycle that governs the soil-plant system [4]. As a matter of fact, the development of nitrogen-based fertilization has become essential for improving production yields as well as agricultural product quality, for example in the frame of wheat culture [5,6].

From another point of view, the excessive use of nitrogen-based fertilizers in modern farming leads today to a worldwide disruption of the nitrogen cycle: atmospheric and hydrological flows of nitrogen no longer compensate and are finally responsible for the degradation of ecosystems through soil leaching, eutrophication of fresh and marine waters, pollution of groundwaters and drinking waters, emission of ammoniac and nitrogen-oxide based gas,… [7-10] In order to guard against the consequences of agriculture on environment and health, regulations and standards were introduced at a worldwide scale and limit concentrations were defined for ammonium NH_4^+ and nitrate NO_3^- ions in soils. This policy implies the development of analytical methods in order to measure ionic concentrations in soil samples. In this context, the first bottleneck was related to sampling techniques [11]. Firstly, they should allow measurements representative of the studied agricultural parcel, while preventing any interferences from soil microorganisms. Secondly, samples must be kept unmodified

during transport from field to lab. Thirdly, to be finally analysed, soil samples have to be diluted into aqueous solutions without changing their chemical composition [12].

Starting from water-based liquid samples, different analysis techniques were developed in order to measure ammonium NH_4^+ ions as well as nitrate NO_3^- ions concentrations: UV spectrophotometry [13], ion chromatography in liquid phase [14], chemical and electrochemical techniques [15,16]. These last techniques are of particular interest since they allow the development of integrated chemical/electrochemical sensors based on ion-sensitive electrodes (ISE) and/or ion-sensitive field effect transistors (ISFET). Thus, potentiometric, amperometric or impedimetric detection methods were thoroughly developed for the detection of nitrogen-based ions [16]. Since the ammonium NH_4^+ ion has no real electroactivity in water-based solutions, potentiometry was mainly proposed for its detection, focusing mainly on nonactin as ionophore [17] and leading to the realization of solid-state microsystems in the frame of environmental analysis [18-27]. Concerning the nitrate NO_3^- ion, competing development paths were considered since its detection is possible using amperometric detection techniques, based on the reduction phenomena on different electroactive surface [28-35], as well as potentiometric ones, based on the use of varied ionophores/ion-sensitive-membranes [18-20, 23-27, 36-38]. Applied to soil analysis, these works led to two different approaches: the "on the go" detection associated with the embedding of electrochemical sensors on agricultural vehicles [39-42], and the "in situ" detection associated with the burying of electrochemical (micro)sensors in fields [43-47].

This paper deals with the development of pNH_4-ISFET and pNO_3-ISFET microsensors for aqueous solution analysis and soil analysis. It proposes the adaptation of a generic pH-ChemFET (pH-sensitive chemical field effect transistor) platform for ion detection thanks to fluoropolysiloxane-based ion-sensitive layers. While dealing with wheat culture application, it focuses on the detection performances optimization in the frame of the "in situ" soil detection approach.

2. Experimental

2.1 Microdevice fabrication

Silicon technologies were used in order to mass integrate microelectrodes as well as pH-sensitive chemical field effect transistors on the same chip (figure 1), according to microfabrication processes previously studied [48,49]. Thus, the proposed technological process can be described briefly as following (figure 2):

- step n°1: field oxidation (800 nm)
- step n°2: field oxide opening (photomask 1) and P-well implantation (boron)
- step n°3: field oxide opening (photomask II) and P++ guard ring implantation (boron)
- step n°4: field oxide opening (photomask III) and N++ Source and Drain implantation (arsenic)
- step n°5: gate opening (photomask IV) and deposition of a SiO_2(50nm)/Si_3N_4(50 nm) insulative layer
- step n°6: contact opening (photomask V)
- step n°7: Ti(20nm)/Pt(150nm) metallization for contact/microelectrode fabrication (photomask VI)
- step n°8: epoxy dry film wafer-level passivation (photomask VII)

Thus, P-well, N-channel, SiO_2/Si_3N_4-gate, pH-sensitive chemical field effect transistors (pH-ChemFET) were fabricated on 4-inch, (100)-oriented, N-type (500 Ω.cm) silicon wafers. Furthermore, thanks to the penultimate technological step, associated to a titanium/platinum metallization lift-off (see below), a specific lithographic mask was used in order to fabricate simultaneously pH-ChemFET contact pads as well as platinum-based microelectrodes Pt-µE (for future measurement of soil conductivity). At least, a wafer-level passivation was performed using the photosensitive DF-1050 epoxy dry film (purchased from EMS company) [50], defining the

microelectrode active surfaces and leaving the pH-ChemFET sensitive zone uncovered for the future integration of ion-sensitive layers.

The multi-sensor devices were manufactured on 6.7 × 5.3 mm^2 chips. These chips were stuck on specifically-coated printed circuit board using an epoxy insulating glue. After wire bonding, packaging was finally performed at the system level using a silicone glop-top in order to adapt the final sensor to the detection in liquid phase (figure 3).

2.2 Integration of ion-sensitive membrane for the fabrication of FET-based sensors

Ion detection was investigated using fluoropolysiloxane polymer (730 FS FPSX purchased from Dow Corning) [51-52]. This polymer was chosen according to previous results [53-54] since, requiring no additional surface treatment it allows good adhesion properties on silicon-based films, and therefore important lifetimes for the associated ion-sensitive layers. Moreover, since fluorosilicone-based coatings, were shown to be good anti-biofouling candidates in the frame of marine application [55], the FPSX polymer could ensure higher lifetime in soils for ion-sensitive layers.

The initial polymeric solution was made of 200 mg of FPSX centrifuged in 1.5 mL of tetrahydrofuran (to eliminate the binder that causes non-optimal functioning). Except for the NI-V (see hereafter) purchased form Santa Cruz Biotechnology, all chemical reagents were purchased from Sigma-Aldrich. For the NH_4^+-sensitive layer, 3.5 mg of nonactin (used as ionophore) and 1.5 mg of "potassium tetrakis(4-chlorophenyl) borate)" KTpClBP ionic additive were diluted into 95 mg of the FPSX-based solution to improve ion exchanging properties, selectivity and lifetime [16, 17, 51-52]. In the same way, for the NO_3^--sensitive one, three ionophores were studied, e.g. tridodecylmethylammonium nitrate (TDMAN), nitrate ionophore V (NI-V) and tetradodecylammonium nitrate (TDDAN), while using two different ionic additives: potassium tetrakis[3,5-bis(trifluoromethyl)phenyl] borate (KTFBP) and tridodecylmethylammonium chloride

(TDMAC). Preparing the initial FPSX-based polymeric solution as previously, the different NO_3^--sensitive layers were developed according to the following dilutions:

matrix #1: 3 mg of TDMAN and 2.5 mg of KTFBP diluted into 94.5 mg of FPSX solution,

matrix #2: 1.8 mg of NI-V and 1.1 mg of TDMAC diluted into 97.1 mg of FPSX solution,

matrix #3: 4 mg of TDDAN and 2.4 mg of KTFBP diluted into 93.6 mg of FPSX solution.

In all cases, ion-sensitive solutions were mixed in an ultrasonic bath (duration: 30 minutes) to insure homogeneity, and was finally deposited by dip coating using a Hamilton micro-syringe (volume: 5 mm^3) installed on a micrometric positioner. Finally, the reticulation reaction was performed at ambient temperature thanks to atmospheric moisture. Mimicking previous results while using low solution volumes (0.1 mm^3) [53], the dip coating process was automatized in order to ensure repeatability and reproducibility. Thus, ion-sensitive, FPSX-based, quasi-semi-ellipsoidal membranes were deposited precisely (deposition accuracy: 50 µm) with dimensions (diameter: 1100 ± 100 µm, height: 7 ± 1 µm) compatible with the pH-ChemFET sensitive zone (figure 4).

According to this ultimate technological step (step n°9: dip-coating deposition of ion-sensitive FPSX-based layers), the SiO_2/Si_3N_4 pH-sensitive ChemFET chips were adapted to ion detection, leading to the realisation of SiO_2/Si_3N_4/FPSX NH_4^+-sensitive and NO_3^--sensitive field effect transistors respectively, called pNH_4-ISFET and pNO_3-ISFET hereafter (figure 2).

2.3 Electrochemical characterization in liquid phase and soil measurements

The different field-effect devices, i.e. pH-ChemFET, pNH_4-ISFET and pNO_3-ISFET, were characterized using a specific "source-drain follower" measurement interface, called ChemFET-meter hereafter. Thus, during measurement experiments, the Gate-Source voltage V_{GS} of the FET-based microsensors was monitored continuously while in saturation mode thanks to constant Drain-

Source voltage V_{DS} and Drain-Source current I_{DS} (typically V_{DS} = 2 V and I_{DS} = 0.1 mA). A commercial calomel reference electrode (XR110 model from Radiometer Analytical) was used to bias the analysed sample solution to the mass ($V_G = 0$). For soil analysis, a specific burying procedure was used for ensuring electrical contacts while preventing any undesired breakage.

Concerning pH-ChemFET devices, titration experiments using hydrochloric acid (HCl: 10^{-2} M) and tetra-methyl-ammonium hydroxide (TMAH: 10^{-1} M) were performed with a background electrolyte (CH_3COOLi 0.1 M) solution to fully study their pH detection properties. Their sensitivities to alkaline ions was studied by successive adding of KCl or NaCl solutions in a buffer solution (pH = 4.66 ± 0.1 pH).

For pNH_4-ISFET and pNO_3-ISFET devices, detection properties in liquid phase were also studied in deionized water (resistivity > 18 MΩ.cm) while increasing regularly the [NH_4^+] and [NO_3^-] concentrations (maximal range: 10^{-8} M – 10^{-2} M) thanks to successive additions of ammonium nitrate NH_4NO_3. Solutions with different specific salt concentrations (KCl, NaCl, $CaCl^2$, $MgSO_4$ and CH_3COOLi) were also studied and potentiometric selectivity coefficients were found out according to the fixed interference method (FIM) [56].

Then, soil analysis was performed by burying the different ChemFET-based sensors into real samples corresponding to two different clay-silt matrices (provided by the Agronutrition company and analysed thanks to the pH-H_2O ISO10390 norm): an acidic one (pH = 4.7 ± 0.1) and an alkaline one (pH = 8.3 ± 0.1). In all cases, a commercial calomel reference electrode (XR110 model purchased from Radiometer Analytical) was used to applied the Gate voltage to the soil sample. After calibrating the pH-ChemFET sensors in three buffer solutions (4, 7 and 10), pH measurements were first performed to check their ability for soil measurement, while considering relative moisture (RM) ranging from 40 to 100% (figure 5).

Finally, ion analysis was also studied in real samples using the acidic clay-silt matrix, characteristic of wheat cultures in the south-west of France. For the NH_4^+ ion, the nitrogen mineralization due to soil micro-organisms was activated thermally to alter biologically the soil

samples. Otherwise, the NH_4^+ ion, the NO_3^--ion detection was performed while modifying soil samples to obtain nitrate concentrations ranging from 0.4 to 10 mM. In both cases, SMS19.21.05F lysimeters (purchased from Rhizon) were used to extract liquid samples from the studied earthen pots. These liquid samples were finally characterized by ionic chromatography using Dionex ICS-5000+ (anions) and DX-120 (cations) equipments. All chemical products were purchased from Sigma-Aldrich and all experiments were done at ambient temperature (~ 21°C).

3. Results and discussion

3.1 pH-ChemFET characterization

The pH detection properties of the SiO_2/Si_3N_4 pH-ChemFET devices were validated by HCl/TMAH titration experiments (results not shown). In a standard way, the developed technology is characterized by a quasi-Nernstian response (sensitivity: 55 ± 1 mV/pH) with no hysteresis on the [2 – 12] pH range, low temporal drift (< 1 mV/day) and long lifetime (more than 6 months). This is associated to the ChemFET process quality as well as to the ability of pH-ChemFET sensors to be used for long-term applications. Nevertheless, it should be mentioned that the studied pH-ChemFET batch was characterized by a detection sensitivity around 51 ± 1 mV/pH. Since this lower sensitivity should be related to a non-stoichiometric silicon nitride film, it will have no influence on the pNH_4- and pNO_3-ISFET detection properties but the value will be considered accordingly hereafter, highlighting the ability of the ChemFET technology to cope with real and in-situ soil analysis.

Concerning their sensitivities to alkaline ions, similar results were obtained for both sodium Na^+ and potassium K^+ ions. On one hand, for the lowest concentrations (lower than 10^{-3} M), there was no influence on the pH-ChemFET response. On the other hand, for the highest concentrations (higher than 10^{-3} M), linear analytical responses were found, evidencing sensitivities around 7.5 ± 0.5 mV/decade [57] (results not shown). Nevertheless, in the frame of soil analysis applied to

agriculture, since alkaline ion concentrations are generally lower than 10^{-3} M, their interference will be finally negligible on pH measurement.

3.2 pNH_4-ISFET and pNO_3-ISFET characterization

In the following, the nitrogen-based ion detection was studied while focusing on concentration ranges compatible with soil analysis: [10^{-5} – 10^{-3} M] for pNH_4 and [10^{-4} – 10^{-2} M] for pNO_3 [3].

Concerning the detection of the ammonium NH_4^+ ion, only nonactin was studied as ionophore while using a FPSX-based polymer matrix. As expected for cations, the pNH_4-ISFET output voltage decreased with the [NH_4^+] concentration increase (figure 6), enabling the definition of the sensor analytical response (figure 7). It appears that the FPSX-based pNH_4-ISFET is characterized by a quasi-Nernstian variation in the [$10^{-2.5}$ – 10^{-5} M] concentration range (sensitivity estimated for nine different sensors: 56 ± 1 mV/pNH_4). It should be mentioned that the measurement discontinuities / transitions evidenced on figure 6 are related to the experimental transfer from one liquid sample to another. These rough data were not treated mathematically, allowing to characterize the sensor transient response. As a result, the pNH_4-ISFET response time was found around two minutes and, after stabilization, its measurement accuracy was estimated to ± 2.5 mV, i.e. to ± 0.05 pNH_4. Such response time value will have no influence for real and in-situ soil analysis since concentration variations in soil occurs on more important time scales (typically few hours or few days).

Then, measurement interferences were estimated for the main soil cations: potassium K^+, sodium Na^+, lithium Li^+, calcium Ca^{2+} and magnesium Mg^{2+} (figure 8). According to the various interfering ions, the different pNH_4-ISFET analytical responses were largely shifted. This phenomenon should be related to interfering ion trapping into the nonactin-based FPSX matrix [17]. For the Na^+ and K^+ ions, interferences were also responsible for a sensitivity decrease (towards 47 and 42.5 mV/pNH_4 respectively). In order to go further, the different potentiometric selectivity coefficients were estimated using the fixed interference method (FIM) (table 1). Except for the K^+

ion, excellent selective properties were obtained while compared to results from literature [58-61], mainly due to the choice of the 730 FS fluoropolysiloxane polymer. In the case of the potassium ion, the Log $K(NH_4^+, K^+)$ value was estimated to -1.2. As previously shown [17], such result should be related directly to the nonactin ionophore. Whereas Na^+ ions are rarely present in the frame of agriculture, only K^+ ion interferences will have to be considered in field applications but it should not be a major bottleneck for the monitoring of soil nitrogen cycle using FPSX-based pNH_4-ChemFET sensors.

Concerning the detection of the nitrate NO_3^- ion, the FPSX-based polymer matrix was studied for the integration of three different ionophores: tridodecylmethylammonium nitrate (TDMAN), nitrate ionophore V (NI-V) and tetradodecylammonium nitrate (TDDAN). In all cases and as expected for anions, the $[NO_3^-]$ concentration increase is responsible for the pNO_3-ISFET output voltage increase (figure 9, associated to the TDDAN matrix). Thus, sensor analytical responses were defined according to the studied matrices (figure 10, associated to the TDDAN matrix). In all cases, the FPSX-based pNO_3-ISFET were associated to quasi-Nernstian curves while evidencing the following characteristics (estimated for three different sensors):

matrix #1 (TDMAN): sensitivity: 53 ± 1 mV/pNO_3 on in the [$10^{-1.5}$ – $10^{-4.5}$ M] concentration range,

matrix #2 (NI-V) sensitivity: 56 ± 1 mV/pNO_3 on in the [$10^{-1.5}$ – $10^{-4.5}$ M] concentration range,

matrix #3 (TDDAN): sensitivity: 56 ± 1 mV/pNO_3 on in the [$10^{-1.5}$ – $10^{-5.5}$ M] concentration range.

As previously, the rough data analysis allowed to characterize the ISFET device transient response (figure 9, associated to the TDDAN matrix). Consequently, the pNO_3-ISFET measurement

accuracy was estimated to ± 1 mV, i.e. to ± 0.02 pNO_3, and its response time to around two minutes (still negligible if compared to concentration variations time scales in soil).

Interferences of the main soil anions (chloride Cl^-, acetate CH_3COO^-, dihydrogen phosphate $H_2PO_4^-$, sulphate SO_4^{2-}, and phosphate PO_4^{3-}) were also estimated. Whereas the different nitrate-sensitive matrices were characterized by similar detection sensitivities and ranges (see below), the interference measurement studies showed degraded analytical responses for the TDMAN-based ion-sensitive matrix as well as for the NI-V-based one (results not shown). Therefore, in the following, focus will be done on the TDDAN-based matrix (figure 11). As previously, large potentiometric shifts were evidenced for the pNO_3-ISFET analytical responses, as a result of interfering ion trapping phenomena associated to the TDDAN ionophore. However, according to measurement accuracy, quasi-Nernstian pNO_3 sensitivities were still evidenced whatever the interfering ions.

Then, the fixed interference method was also used to determine the potentiometric selectivity coefficients associated to the different studied anions. Table 2 compares finally the so-obtained values to results extracted from literature [62-64], emphasizing the use of the 730 FS fluoropolysiloxane polymer. According to table 2, it should be also noted that, although TDDAN is an ion exchanger, selectivity towards phosphate PO_4^{3-} ions is surprisingly worse than for the sulphate SO_4^{2-} ion, in disagreement with the Hofmeister series [65]. Moreover, according to literature [62-64], the replacement of the poly-vinyl-chloride (PVC) polymer by the fluoropolysiloxane (FPSX) one as well as the use of the KTFBP ionic additive did not generate an improvement in selectivity (in fact, this additive is primordial for the stability of the ISFET sensor in solution, result not shown). As a matter of fact, for both polymers, results obtained with the TDDAN ionophore remain excellent. In the frame of agricultural applications, chloride Cl^- appears to be the main interfering ion but its potentiometric selectivity coefficient Log $K(NO_3^-, Cl^-)$ around -2.5 should be sufficient for nitrate ion analysis in soil.

Thus, according to sensitivity and selectivity results, the TDDAN-based FPSX matrix appears to be the best nitrate-sensitive layer, and should be fully compatible with the NO_3^- ion detection in soils using ChemFET sensors.

3.3 Application of the ChemFET technology to soil analysis

The first soil analysis concerned the standard SiO_2/Si_3N_4-pH-ChemFET technology while considering two different clay-silt soil matrices: acidic (pH ≈ 4.7) and alkaline (pH ≈ 8.3). Considering both soil samples, pH-ChemFET devices were buried into earthen pots for relative moistures (RM) ranging from 40% to 100%, in agreement with soil-plant system and agriculture considerations [4]. During pH measurements, the ChemFET-meter experimental curves showed often initial transient variations (result not shown). Such phenomenon should be related to the electrical contact establishment between the pH-ChemFET sensitive structure and the soil matrix. Nevertheless, a steady-state regime was evidenced after thirty minutes in soil, enabling the determination of a constant output voltage whatever the relative moisture values (table 3). This demonstrate that such soil RM levels allow the creation of a liquid interface compatible with the Electrolyte-Insulator-Semiconductor detection structure. So, pH-ChemFET sensor results were quite stable and in good agreement with initial pH analyses. Whatever the RM values, measurement errors were lower than 0.5 pH and the acidic and alkaline soils were respectively associated to pH values around 4.9 ± 0.3 and 8.1 ± 0.3.

Then, experimental studies dedicated to pH-ChemFET drift and lifetime in the acidic clay-silt soil (pH = 4.7) were performed on a six-month period, while keeping constant the soil relative moisture constant around 75%, representative of a wheat culture applications [5] (figure 12). Linear output voltage variations were evidenced, with a potential shift around + 100 mV on a 165-day duration (temporal drift: ~ 0.6 mV/day or ~ 0.012 pH/day). Such phenomenon could be related to an effective pH variation of the clay-silt matrix on the six-month duration, but also to a drift of the pH-

ChemFET device. In order to go further, HCl/TMAH titration experiments were performed on the pH-ISFET sensors to study their analytical responses after six months of use in earth (result not shown). Linear curves were still obtained, evidencing similar sensitivity (~ 51 mV/pH) as well a positive threshold voltage shift around + 35 mV. So, considering the previous global potential shift (~ 100 mV), around 65 mV should be associated to an effective pH increase of the clay-silt soil matrix, and the pH-ChemFET drift was finally estimated to 0.2 mV/day (or 0.004 pH/day). Last but not least, the pH-ChemFET sensor lifetime in soil was found to be higher than six months, in agreement with wheat culture specifications.

As a matter of fact, these preliminary experiments highlight the potential of the ChemFET technology for in-situ soil analysis on a six-month growth period, even in rain conditions or dry weather periods. Compared to the agriculture-related current methods, that require a time-consuming analysis of a soil extract, such technology offers the possibility of an almost immediate result on site, with sufficient accuracy in the frame of precision farming.

3.4 In-situ soil analysis using pNH_4-ISFET and pNO_3-ISFET sensors

In-situ experiments were systematically performed while using the acidic clay-silt soil (pH = 4.7 ± 0.1, RM ≈ 75%, see below), characteristic of wheat culture in the south-west of France.

The first study was dedicated to the measurement of the ammonium ion concentration. In order to do so, one earth pot was incubated at 38°C in an oven in order to activate the nitrogen mineralization due to soil micro-organisms whereas the second one was maintained at 4°C in a fridge in order to prevent it. After one month, a pNH_4-ISFET was used to characterized the different pots according to the following routine: calibration into NH_4NO_3 solutions (10^{-4} M and 10^{-3} M), analysis of the NH_4^+-rich and NH_4^+-poor soil samples after burying (two times), and final calibration into NH_4NO_3 solutions (10^{-4} M and 10^{-3} M), and its output voltage was monitored accordingly (figure 13). Thanks to the initial calibration steps (output voltage shift around 50 mV), the pNH_4-ISFET

operation was validated. Between each burying steps, there is clearly a drift in the sensor signal. Again, this should be related to transient regime due the improvement of the contact impedances between the sensor and the soil matrix. Nevertheless, the two-time analysis of the NH_4^+-rich and NH_4^+-poor earth pots showed another voltage shift estimated around 40 mV. The final calibration step showed lastly that the pNH_4-ISFET is still operational and that the previous values are correlated to effective variations of the ammonium ion concentration [NH_4^+]. In all, the monitoring of the nitrogen mineralization due to soil micro-organisms was demonstrated and the ISFET behaviour seemed unaffected by any biofouling phenomena or associated ones.

Compared to the pNH_4-ISFET calibration procedure in 10^{-4} M and 10^{-3} M solutions (sensitivity: ~ 50 mV/pNH_4), the ammonium ion concentrations of the NH_4^+-poor and NH_4^+-rich samples were respectively estimated to 150 ± 50 µM and 800 ± 100 µM (table 4). Nevertheless, such results have to be analysed in a critical way by considering the interference of the potassium ion concentration (see table 2). According to our previous results (see §3.2, Log K(NH_4^+, K^+) ≈ -1.2), the final [NH_4^+] concentrations of both soil samples could be respectively estimated to approximately 150 µM and 700 µM, in quite good agreement with measurement performed by ionic chromatography analysis on lysimeters liquid samples (table 4).

All in all, even if drift phenomena involve important measurement errors, these experiments allowed to discriminate fully two levels of soil mineral nitrogen, and to analyse, on a monthly basis, the temperature-stimulated activity of micro-organisms in clay-silt soils.

Then, the nitrate ion detection was also studied. First, using the standard method based on soil sample dilution into pure water, the NO_3^- ion and the Cl^- ion concentrations were respectively estimated to 0.4 mM and 2.5 mM for the acidic clays-silt soil. According to this result and considering that nitrate ions are chemically available in the soil matrix, four earth pots were prepared with different concentrations [NO_3^-] and were characterized by ionic chromatography thanks to soil-related liquid samples. Finally, a pNO_3-ISFET was used to characterized the different pots according

to the following routine: calibration into NH_4NO_3 solutions (10^{-3} M and 10^{-2} M), analysis of the four soil samples after burying (four times), and final calibration into NH_4NO_3 solutions (10^{-3} M and 10^{-2} M).

Results show a quite good agreement between theoretical [NO_3^-] concentrations and measured ones (table 5). They show that ISFET sensors tends to overestimate the nitrate content, certainly due to the Cl^- chloride ion interferences. Nevertheless, a quite good and monotonous agreement was evidenced, demonstrating the ability of ISFET sensors to measure fully nitrate NO_3^- ion concentration in soil.

Finally, the ISFET sensor lifetime in soil has to be studied. In this case, in order to prevent any deterioration of the FPSX-based ion-sensitive membranes, ISFET sensors were buried into earthen pots containing the acidic clay-silt soil saturated with water (pH = 4.7 ± 0.1, RM ≈ 100%). Then, during six months, they were periodically and cautiously removed, cleaned into pure water, calibrated into NH_4NO_3- based aqueous solutions to estimate their detection properties, and finally buried again into their earthen pots. Since linear analytical responses were systematically obtained, results were finally analysed according to their detection sensitivity as well as their output voltage for a 10^{-4} M NH_4NO_3 solution ($pNH_4 = pNO_3 = 4$). Thus, it appeared that, for both pNH_4-ISFET and pNO_3-ISFET devices, detection responses remained quasi-Nernstian and their sensitivity decreased from 56 to 50 mV/decade during the six-month burying period.

Contradictory results were rather obtained for the temporal drift analysis thanks to the reference value obtained at $pNH_4 = pNO_3 = 4$ (results not shown). On one hand, for the pNH_4-ISFET, no real potential shift was evidenced on a six-month burying period (output voltage: 1,18 ± 0.02 V). Since the sensor was not in use during the burying period, this "zero" temporal drift value cannot be compared to the previous one determined for pH-ISFET in clay-silt soil (cf. §3.3). Nevertheless, this result demonstrates that the lifetime of fluorosiloxane-based ion-sensitive layers is also higher than six months, and that the FPSX-based pNH_4-ISFET sensors could be used for soil monitoring on a six-month growth period. On another hand, for the pNO_3-ISFET, a huge potential shift was found,

leading to major dysfunctions. According to the previous results (see below), this huge drift should be related to the physico-chemical integration of the TDDAN ionophore into the FPSX membrane. Besides, a similar phenomenon was also obtained in liquid phase (results not shown). As a matter of fact, this demonstrates that the improvement of NO_3^--sensitive layers still remains a bottleneck for the development of pNO_3 potentiometric ChemFET-based sensors.

4. Conclusion

Silicon-based technologies were used to develop ChemFET-based sensors for the nitrogen cycle monitoring in soil. Thus, focusing on nonactin and tetradodecylammonium nitrate (TDDAN) ionophores respectively, pH-ChemFET devices were adapted to the detection of ammonium NH_4^+ and nitrate NO_3^- ions thanks to fluoropolysiloxane-based, ion-sensitive membranes deposited by dip-coating. The pNH_4-ISFET and pNO_3-ISFET were characterized by quasi-Nernstian detection properties (sensitivity: ~ 56 mV/decade) in a [10^{-2} – 10^{-5} M] concentration range adapted to soil analysis. Their selectivity properties were also studied, evidencing the potassium K^+ and chloride Cl^- ions as the main interfering species respectively (potentiometric selectivity coefficients: Log $K(NH_4^+, K^+) \approx -1.2$ and Log $K(NO_3^-, Cl^-) \approx -2.5$).

Focusing on the "in situ" detection approach, soil analysis was finally performed during burying periods of six-month, as required for nitrogen-based fertilization procedure in the frame of agriculture applications. Whatever their acid/basic and moisture characteristics, pH-ChemFET were found to be fully compatible with clay-silt soil analysis, evidencing stable analytical responses for six months (temporal drift: ~ 0.004 pH/day). Similar studies were also done for the nitrogen-based ion-sensitive sensors. So, pNH_4-ISFET were used for analysing, on a monthly basis, the nitrogen mineralization due to temperature-stimulated activity of micro-organisms in soil. In addition, pNO_3-ISFET were successfully used to measure nitrate ion concentration [NO_3^-] in soil. Overall, the ability of FPSX-based ISFET sensors to operate in-situ in clay-silt soil during a six-month period was demonstrated.

Nevertheless, some bottlenecks were also highlighted. The first one is minor since it is related to the potassium ion interferences on the intrinsic detection properties of the nonactin ionophore and therefore on the pNH_4-ISFET analytical responses. Since there is no real alternative in terms of ionophore, this phenomenon should be only considered for future applications of pNH_4-ChemFET sensors in soils. The second one is related to physico-chemical properties of the TDDAN ionophore into the FPSX polymeric membrane. Even if pNO_3-ISFET were successfully developed in the frame of soil analysis, major dysfunctions were finally evidenced after few days, preventing their efficient use for long durations. Consequently, research works have to be continued. They have to concern the improvement of FPSX-based nitrate-sensitive layers. Nevertheless, in the frame of the "in situ" approach for modern farming, efforts must also be focused on the development of a functional (micro)system analysis, fully compatible with the soil analysis. Thus, it should be possible to monitor the nitrogen cycle in soils or to study the influence of nitrogen-based fertilizers in fields.

Acknowledgements

This project was financially supported by the French "Fonds Unique Interministériel" and the French "Midi-Pyrénées Région" (FUI project, AAP 16, n°F1401015M). The technological realisations and associated research works were partly supported by the French RENATECH network.

References

[1] M. Hawkesford, "Chapter 6: Functions of macronutrients", in "Marschner's mineral nutrition of higher plants" (3rd Edition), P. Marschner, Ed. San Diego: Academic Press (2012), 135-189

[2] M. Andrews, J.A. Raven, P.J. Lea: "Do plant needs nitrate ? The mechanisms by which nitrogen forms affect plants", *Annals of Applied Biology*, 163 (2013) 174-199

[3] A.G. Owen, D.L. Jones: "Competition for amino acids between roots and rhizosphere microorganisms and the role of amino acids in plant N acquisition", *Soil Biology and Biochemistry*, 33 (2001) 651-657

[4] H.J. Di, K.C. Cameron: "Nitrate leaching in temperate agroecosystems: sources, factors and mitigating strategies", *Nutrition Cycle Agroecosystems*, 64 (2002) 237-256

[5] http://www.fao.org/faostat/, FAOSTAT, Food and Agriculture Organization of the United Nations

[6] Z. Liang, K.F. Bronson, K.R. Thorp, J. Mon, M. Badaruddin, G. Wang: "Cultivar and N fertilizer rate affect yield and N use efficiency in irrigated durum wheat", *Crop Science*, 54 (2014) 1175-1183

[7] G. Billen, J. Garnier, L. Lassaletta: "The nitrogen cascade from agricultural soils to the sea: modelling nitrogen transfers at regional watershed and global scales", *Philosophical transactions of the Royal Society B: Biological sciences*, 105 (2010) 1141-1157

[8] G. Billen, A. Beusen, L. Bouwman, J. Garnier: "Anthropogenic nitrogen autography and heterotrophy of the world's watersheds: past, present and future trends", *Global Biogeochemical cycles*, 24 (2010) GB0A11, 1-12

[9] http://ec.europa.eu/environment/water/water-nitrates/reports.html, Report COM(2002)407, Environment, European Commission

[10] C. Masclaux-Daubresse, F. Daniel-Vedele, J. Dechorgnat, F. Chardon, L. Gaufichon, A. Suzuki: "Nitrogen uptake, assimilation and remobilization in plants: challenges for sustainable and productive agriculture", *Annals of Botany*, 105 (2010) 1141-1157

[11] A.R. Conklin Jr., "Chapter 7: Soil and soil solution sampling, sample, transport and storage", in "Introduction to soil chemistry", John Wiley & Sons Inc. (2014) 135-158

[12] D.G. Maynard, Y.P. Kalra, J.A. Crumbaugh, "Chapter 6: Nitrate and exchangeable ammonium nitrogen", in "Soil sampling and methods of analysis" (2nd edition), M.R. Carter and E.G. Gregorich, Ed., CRC press (2007) 71-80

[13] R.J. Norman, J.C. Erdberg, J.W. Stucki: "Determination of nitrate in soil extracts by dual-wavelength ultraviolet spectrophotometry", *Soil Science Society of America Journal*, 49 (1985) 1182-1185

[14] R. Michalski, I. Kurzyca: "Determination of nitrogen species (nitrate, nitrite and ammonium ions) in environmental samples by ion chromatography", *Polish Journal of Environmental Studies*, 15 (2006) 5-18

[15] C. Jimenez-Jorquera, J. Orozco, A. Baldi: "ISFET-based microsensors for environmental monitoring", *Sensors*, 10 (2010), 61-83

[16] M.A. Parvez Mahmud, F. Ejeian, S. Azadi, M. Myers, B. Pejcic, R. Abassi, A. Razmjou, M. Asadnia: "Recent progress in sensing nitrate, nitrite, phosphate and ammonium in aquatic environments", *Chemosphere*, 259 (2020) 127492

[17] M. Cuartero, N. Colozza, B.M. Fernandez-Pérez, G.A. Crespo: "Why ammonium detection is particularly challenging but insightful with ionophore-based potentiometric sensors – an overview of the progress in the last 20 years", Analyst, 145 (2020) 3188-3210

[18] M. Chudy, W. Wroblewski, A. Dybko, Z. Brzozska: "Multi-ion analysis on versatile sensor head", *Sensors and Actuators B*, B78 (2001) 320-335

[19] J. Artigas, A. Beltran, C. Jimenez, A. Baldi, R. Mas, C. Dominguez, J. Alonso: "Application of ion field-effect-transistor-based sensors to soil analysis", *Computers and Electronics in Agriculture*, 31 (2001) 281-293

[20] P. Temple-Boyer, J. Launay, I. Humenyuk, T. Do Conto, A. Martinez, C. Bériet, A. Grisel: "Study of front-side connected chemical field effect transistor for water analysis", *Microelectronics Reliability*, 44 (2004), 443-447

[21] I. Humenuyk, B. Torbiéro, S. Assié Souleille, R. Colin, X. Dollat, B. Franc, A. Martinez, P. Temple-Boyer: "Development of pNH_4-ISFET microsensors for water analysis", *Microelectronics Journal*, 37 (2006), 475-479

[22] M. Gutiérrez, V.M. Moo, S. Alegret, L. Leija, P.R. Hernandez. R. Munoz, M. del Valle: "Electronic tongue for the determination of alkaline ions using a screen-printed potentiometric sensor array", *Microchimica Acta*, 163 (2008), 81-88

[23] N. Pankratova, G.A. Crespo, M.G. Afshar, M.C. Crespi, S. Jeanneret, T. Cherubini, M.-L. Tercier-Waeber, F. Pomati, E. Bakker: Potentiometric sensing array for monitoring aquatic systems", *Environmental Science: Process and impacts*, 17 (2015) 906-914

[24] J. Choosang, A. Numnuam, P. Thavarungkul, P. Kanatharana, T. Radu, S. Ullah, A. Radu: Simultaneous detection of ammonium and nitrate in environmental samples using on ion-selective electrode and comparison with portable colorimetric assays", *Sensors*, 18 (2018) 3555-3566

[25] N.T. Garland, E.S. Mc Lamore, N.D. Cavallaro, D. Mendivelso-Perez, E.A. Smith, D. Jing, J.C. Claussen: "Flexible laser-induced graphene for nitrogen sensing in soil. *ACS Applied Materials Interfaces*, 10 (2018) 39124–39133

[26] J. Schwarz, K. Trommer, M. MertigHauser: "Solid-Contact Ion-Selective Electrodes Based on Graphite Paste for Potentiometric Nitrate and Ammonium Determinations", *American journal of analytical chemistry*, 9 (2018) 591-601

[27] J. Gallardo-Gonzalez, A. Baraket, S. Boudjaoui, T. Metzner, F.Hauser, T. Rößler, S. Krause, N. Zine, A. Streklas, A. Alcácer, J. Bausells, A. Errachid: "A fully integrated passive microfluidic Lab-on-a-Chip for real-time electrochemical detection of ammonium: sewage applications", *Science of the total environment*, 653 (2019) 1223-1230

[28] M. Badea, A. Amine, G. Palleschi, D. Moscone, G. Volpe, A. Curulli: "New electrochemical sensors for the detection of nitrites and nitrates", *Journal of electrochemical analysis*, 509 (2001), 66-72

[29] X.-L. Zhang, J.-X. Wang, Z. Wang, S.C. Wang: " Improvement of amperometric sensor used for determination of nitrate with polypyrrole nanowires modified electrode", *Sensors*, 5 (2005), 580-593

[30] J.T. Matsushima, W.M. Silva, A.F. Azevedo, M.R. Baldan, N.G. Ferreira: "The influence of boron content on electroanalytical detection of nitrate using BDD electrodes", *Applied surface science*, 256 (2009), 757-762

[31] M.-P.N. Bui, J. Brockgreitens, A. Snober, A. Abbas: "A dual detection of nitrate and mercury in water using disposable electrochemical sensors", *Biosensors & Bioelectronics*, 85 (2016) 280–286

[32] L.D. Chen, C. Barus, V. Garçon: "Square wave voltammetry measurements of low concentrations of nitrate using Au/AgNPs electrode in chloride solutions", *Electroanalysis*, 29 (2017) 2882–2887

[33] E. Lebon, P. Fau, M. Comtat, M.L. Kahn, A. Sournia-Saquet, P. Temple-Boyer, B. Dubreuil, P. Behra, K. Fajerwerg: "In-situ metalorganic deposition of silver nanoparticles on gold substrate and square wave voltammetry: a highly efficient combination for nanomolar detection of nitrate ions in sea water", *Chemosensors*, 6 (2018), 50-61

[34] S. Zhao, J. Tong, Y. Li, J. Sun, C. Bian, S. Xia: "Palladium-gold modified ultramicro interdigital array electrode chip for nitrate detection in neutral water", *Micromachines*, 10 2019, 223-232

[35] J. Wang, P. Diao: "Simultaneous detection of ammonia and nitrate using a modified electrode with two regions", *Microchemical Journal*, 154 (2020) 104649

[36] L. Campanella, C. Colapicchioni, G. Crescentini, M.P. Sammartino, Y. Su, M. Tomassetti: "Sensitive Membrane ISFETs for Nitrate Analysis in Waters", *Sensors and Actuators B*, B27 (1995) 329-335

[37] W. Tang, J. Ping, K. Fan, Y. Wang, X. Luo, Y. Ying, J. Wu, Q. Zhou: "All-solid-state nitrate-selective electrode and its application in drinking water, *Electrochimica Acta*, 81 (2012) 186–190

[38] A. Calvo-Lopez, E. Arasa-Puig, M. Puyol, J.M. Casalta: "Biparametric potentiometric analytical microsystem for nitrate and potassium monitoring in water recycling processes for manned space missions", *Analytica Chimica Acta*, 804 (2013), 190-196

[39] S. J. Birrell and J. W. Hummel, “Real-time multi ISFET/FIA soil analysis system with automatic sample extraction”, *Computers and Electronics in Agriculture*, 32 (2001) 45–67

[40] V.I. Adamchuk, E.D. Lund, B. Sethuramasamyraja, M.T. Morgan, A. Dobermann, D.B. Marx: "Direct measurement of soil chemical properties on-the-go using ion-selective electrodes", *Computers and Electronics in Agriculture*, 48 (2005) 272–294

[41] K.J. Sibley, T. Astatkie, G. Brewster, P.C. Struik, J.F. Adsett, K. Pruski: "Field-scale validation of an automated soil nitrate extraction and measurement system", *Precision Agriculture*, 10 (2009) 162-174

[42] J.V. Sinfield, D. Fagerman, O. Colic: "Evaluation of sensing technologies for the on-the-go detection of macro-nutrients in cultivated soils", *Computers and Electronics in Agriculture*, 70 (2010) 1-18

[43] J. Artigas, C. Jimenez, S. G. Lemos, A. R. A. Nogueira, A. Torre-Neto, J. Alonso, "Development of a screen-printed thick-film nitrate sensor based on a graphite-epoxy composite for agricultural applications", *Sensors and Actuators B*, B88 (2003) 337–344

[44] M. Futagawa, T. Iwasaki, H. Murata, M. Ishida, K. Sawada: "A miniature integrated multimodal sensor for measuring pH, EC and temperature for precision agriculture", *Sensors*, 12 (2012) 8338–8354

[45] K.L. Tully, R. Weil: "Ion-selective electrode offers accurate, inexpensive method for analyzing soil solution nitrate in remote regions," *Communication in Soil Science and Plant Analysis*, 45 (2014), 1974–1980

[46] W.-O. Caron, M.S. Lamhamedi, J. Viens, Y. Messaddeq: "Practical application of electrochemical nitrate sensor under laboratory and forest nursery conditions", *Sensors*, 16 (2016) 1190-1203

[47] H. Jiang, M.A. Ali, Y. Jiao, B. Yang, L. Dong, "In-situ, real-time monitoring of nutrient uptake on plant chip integrated with nutrient sensor", *Proceedings of the 19th International Conference on Solid-State Sensors, Actuators and Microsystems (TRANSDUCERS 2017)*, 289–292

[48] W. Sant, P. Temple-Boyer, E. Chanié, J. Launay and A. Martinez: "On-line monitoring of urea using enzymatic field effect transistors", *Sensors and Actuators B*, B160 (2011) 59-64

[49] C. Christophe, F. Sékli Belaïdi, J. Launay, P. Gros, E. Questel, P. Temple-Boyer: "Elaboration of integrated microelectrodes for the detection of antioxidant species", *Sensors and Actuators B*, B177 (2013) 350-356

[50] Y. Temiz, A. Ferretti, Y. Leblebici, C. Guiducci: "A comparative study on fabrication techniques for on-chip microelectrodes", Lab on a chip, 12 (2012) 4920-4928

[51] C. Dumschat, S. Alazard, S. Adam, M. Knoll, K. Camman: "Filled fluorosiloxane as matrix for ion-selective membranes", *Analyst*, 121 (1996) 527-529

[52] G. Hogg, O. Lutze and K. Camman: "Novel membrane material for ion-selective field effect transistors with extended lifetime and improved selectivity", *Analytica Chimica Acta*, 335 (1996) 103-109

[53] A. Cazalé, W. Sant, J. Launay, F. Ginot, P. Temple-Boyer: "Study of field effect transistors for the sodium ion detection using fluoropolysiloxane-based sensitive layers", *Sensors and Actuators B*, B177 (2013) 515-521

[54] A. Cazalé, W. Sant, F. Ginot, J.C. Launay, G. Savourey, F. Revol-Cavalier, J.M. Lagarde, D. Heinry, J. Launay, P. Temple-Boyer: "Physiological stress monitoring using sodium ion potentiometric microsensors for sweat analysis", *Sensors and Actuators B*, B225 (2016) 1-9

[55] P. Hu, Q. Xie, C. Ma, G. Zhang: "Silicone-based fouling release coatings for marine antifouling", *Langmuir*, 36 (2020) 2170-2183

[56] Y. Umezawa, K. Umezawa, H. Sato: "Selectivity coefficients for ion-selective electrodes: recommended methods for reporting K_{AB}^{pot} values", *Pure and Applied Chemistry*, 67 (1995) 507-518

[57] B. Hajji, P. Temple-Boyer, J. Launay, T. Do Conto, A. Martinez: "pH, pK and pNa detection properties of SiO_2/Si_3N_4 ISFET chemical sensors", *Microelectronics reliability*, 40 (2000) 783-786

[58] M.S. Ghauri, J.D.R. Thomas: "Poly(vinyl chloride) type ammonium ion-selective electrodes based on nonactin: solvent mediator effects", *Analytical Proceedings including Analytical Communications*, 31 (1994) 181–183

[59] W. Wroblewski, M. Chudy, A. Dybko, Z. Brzozka: "NH_4^+-sensitive chemically modified field effect transistors based on siloxane membranes for flow-cell applications," *Analytica Chimica Acta*, 401 (1999) 105–110

[60] E. Karakus, S. Pekyardimci, and E. Kilic: "A new potentiometric ammonium electrode for biosensor construction", *Artificial Cells, Blood Substitutes and Biotechnology*, 34 (2006) 523–534

[61] M. Novell, M. Parrilla, G. A. Crespo, F. X. Rius, and F. J. Andrade, "Paper-based ion-selective potentiometric sensors", *Analytical Chemistry*, 84 (2012) 4695–4702

[62] W. Wroblewski, M. Chudy, A. Dybko: "Nitrate-selective chemically modified field effect transistors for flow-cell applications", *Analytica Chimica Acta*, 416 (2000) 97–104

[63] T. Masadome, K. Nakamura, D. Iijima, O. Horiuchi, B. Tossanaitada, S;-I. Wakida, T. Imato: "Microfluidic polymer chip with an embedded ion-selective electrode detector for nitrate-ion assay in environmental samples", *Analytical Sciences: The International Journal of the Japan Society for Analytical Chemistry*, 26 (2010) 417–423

[64] L. Zhang, M. Zhang, H. Ren, P. Pu, P. Kong, H. Zhao: "Comparative investigation on soil nitrate-nitrogen and available potassium measurement capability by using solid-state and PVC ISE", *Computers and Electronics in Agriculture*, 112 (2015) 83–91

[65] Y. Zhang, P.S. Cremer: "Interactions between macromolecules and ions: the Hofmeister series", *Current opinion in Chemical Biology*, 10 (2006) 658-663

Tables and figures caption

Table 1: potentiometric selectivity coefficients obtained for different soil-related cations, comparison of pNH_4-ISFET devices with different ion-sensitive polymer-based membranes while focusing on the nonactin ionophore

Table 2: potentiometric selectivity coefficients obtained for different soil-related anions, comparison of pNO_3-ISFET devices with different ion-sensitive polymer-based membranes while focusing on the TDDAN ionophore

Table 3: pH-ISFET measurement in acidic (pH ≈ 4.7) and alkaline (pH ≈ 8.3) clay-silt soil samples characterized by different relative moistures

Table 4: comparison of in-situ pNH_4-ISFET measurements and ionic chromatography analysis of different clay-silt soil pots (pH = 4.7 ± 0.1, RM ≈ 75%) incubated in order to inhibit or activate the nitrogen mineralization due to soil micro-organisms (ionic chromatography was performed on liquid samples extracted by lysimetry)

Table 5: in-situ measurement of clay-silt soil samples (pH = 4.7 ± 0.1, RM ≈ 75%) with different nitrate ion [NO_3^-] concentrations, comparison of the pNO_3-ISFET analysis to ionic chromatography performed on soil-related liquid samples

Figure 1: mass fabrication of SiO_2/Si_3N_4 pH-ChemFET chips using silicon-based technologies

Figure 2: schematic cross section of the proposed ISFET device

Figure 3: integration of pH-ChemFET silicon chips on printed circuit board

Figure 4: dip-coating deposition of the fluoropolysiloxane-based ion-sensitive layer on the SiO_2/Si_3N_4 pH-ChemFET sensitive zone

Figure 5: analysis of clay-silt matrices using ChemFET-based sensors

Figure 6: temporal variations of the pNH_4-ISFET device with increasing $[NH_4^+]$ concentration (studied case: nonactine ionophore and KTpClBP ionic additive in a FPSX-based polymer matrix)

Figure 7: pNH_4-ISFET analytical response in NH_4NO_3 aqueous solutions using a calomel reference electrode (potentiometric measurement accuracy: ± 2.5 mV, studied case: nonactine ionophore and KTpClBP ionic additive in a FPSX-based polymer matrix)

Figure 8: pNH_4-ISFET analytical response in presence of various interfering ions (FIM method) using a calomel reference electrode (potentiometric measurement accuracy: ± 2.5 mV, studied case: nonactine ionophore and KTpClBP ionic additive in a FPSX-based polymer matrix)

Figure 9: temporal variations of the pNO_3-ISFET device with increasing $[NO_3^-]$ concentration (studied case: TDDAN ionophore and KTFBP ionic additive in a FPSX-based polymer matrix)

Figure 10: pNO_3-ISFET analytical response in NH_4NO_3-based aqueous solutions using a calomel reference electrode (potentiometric measurement accuracy: ± 1 mV, (studied case: TDDAN ionophore and KTFBP ionic additive in a FPSX-based polymer matrix)

Figure 11: pNO_3-ISFET analytical response in presence of various interfering ions (FIM method) using a calomel reference electrode (potentiometric measurement accuracy: ± 1 mV, (studied case: TDDAN ionophore and KTFBP ionic additive in a FPSX-based polymer matrix)

Figure 12: temporal drift of a pH-ISFET sensor buried into an acidic (pH = 4.7) clay-silt soil matrix for a six-month period (potentiometric measurement accuracy: ± 1 mV)

Figure 13: monitoring of the pNH_4-ISFET response according to the following routine: calibration into NH_4NO_3 solutions (10^{-4} and 10^{-3} M), burying into NH_4^+-rich and NH_4^+-poor soil pots, final calibration into NH_4NO_3 solutions (10^{-4} and 10^{-3} M)

reference	this work	[58]	[59]	[60]	[61]
polymer-based matrix	FPSX	PVC-NPOE	Siloprene	PVC-DOS	PVC-DOS
ionophore	nonactin	nonactin	nonactin	nonactin	nonactin
Log K(NH_4^+, K^+)	-1.2	-1.4	-1.0	-1.0	-1.2
Log K(NH_4^+, Na^+)	-3.0	-2.2	-2.3	-1.8	-3.0
Log K(NH_4^+, Li^+)	-4.1	-2.1	-2.1	-1.7	-4.7
Log K(NH_4^+, Ca_2^+)	-4.8	-3.4	-3.8	-1.8	-4.7
Log K(NH_4^+, Mg_2^+)	-5.0	-3.4	-3.6	n/a	-3.8

Table 1: potentiometric selectivity coefficients obtained for different soil-related cations, comparison of pNH_4-ISFET devices with different ion-sensitive polymer-based membranes while focusing on the nonactin ionophore

reference	this work	this work	this work	[62]	[63]	[64]
polymer-based matrix	FPSX	FPSX	FPSX	PVC	PVC	PVC
ionophore	TDMAN	NI-V	TDDAN	TDDAN	TDDAN	TDDAN
Log K(NO_3^-, Cl^-)	-1.5	-1.6	-2.5	-2.6	-2.4	-2.4
Log K(NO_3^-, CH_3COO^-)	-2.5	-2.5	-3.8	-	-2.9	-
Log K(NO_3^-, $H_2PO_4^-$)	-2.1	-2.9	-4.2	-3.6	-3.3	-4.4
Log K(NO_3^-, SO_4^{2-})	-2.7	-3.1	-4.5	-4.1	-4.3	-4.8
Log K(NO_3^-, PO_4^{3-})	-	-4.0	-3.2	-	-	-

Table 2: potentiometric selectivity coefficients obtained for different soil-related anions, comparison of pNO_3-ISFET devices with different ion-sensitive polymer-based membranes while focusing on the TDDAN ionophore

Soil relative moisture	40%	60%	80%	100%
pH-ISFET measurement for the acidic clay-silt matrix (pH ≈ 4.7)	5.1 ± 0.1	5.0 ± 0.1	4.7 ± 0.1	4.9 ± 0.1
pH-ISFET measurement for the alkaline clay-silt matrix (pH ≈ 8.3)	8.1 ± 0.1	7.9 ± 0.1	8.3 ± 0.1	8.1 ± 0.1

Table 3: pH-ISFET measurement in acidic (pH ≈ 4.7) and alkaline (pH ≈ 8.3) clay-silt soil samples characterized by different relative moistures

Incubation procedure	1 day at 4°C	30 days at 4°C	1 day at 38°C	30 days at 38°C
pNH_4-ISFET measurement	-	150 ± 50 µM	-	800 ± 100 µM
$[NH_4^+]$ analysis by ionic chromatography	125 ± 25 µM	175 ± 25 µM	275 ± 25 µM	725 ± 25 µM
$[K^+]$ analysis by ionic chromatography	35 ± 10 µM	30 ± 10 µM	125 ± 10 µM	350 ± 10 µM

Table 4: comparison of in-situ pNH_4-ISFET measurements and ionic chromatography analysis of different clay-silt soil pots (pH = 4.7 ± 0.1, RM ≈ 75%) incubated in order to inhibit or activate the nitrogen mineralization due to soil micro-organisms (ionic chromatography was performed on liquid samples extracted by lysimetry)

theoretical nitrate ion concentration [NO_3^-]	0.4 mM	0.8 mM	1.6 mM	10 mM
pNO_3-ISFET measurement	0.4 ± 0.1 mM	1 ± 0.35 mM	3.3 ± 0.4 mM	12.5 ± 2.5 mM
[NO_3^-] analysis by ionic chromatography	0.4 ± 0.05 mM	0.7 ± 0.05 mM	1.8 ± 0.1 mM	10.5 ± 0.5 mM

Table 5: in-situ measurement of clay-silt soil samples (pH = 4.7 ± 0.1, RM ≈ 75%) with different nitrate ion [NO_3^-] concentrations, comparison of the pNO_3-ISFET analysis to ionic chromatography performed on soil-related liquid samples

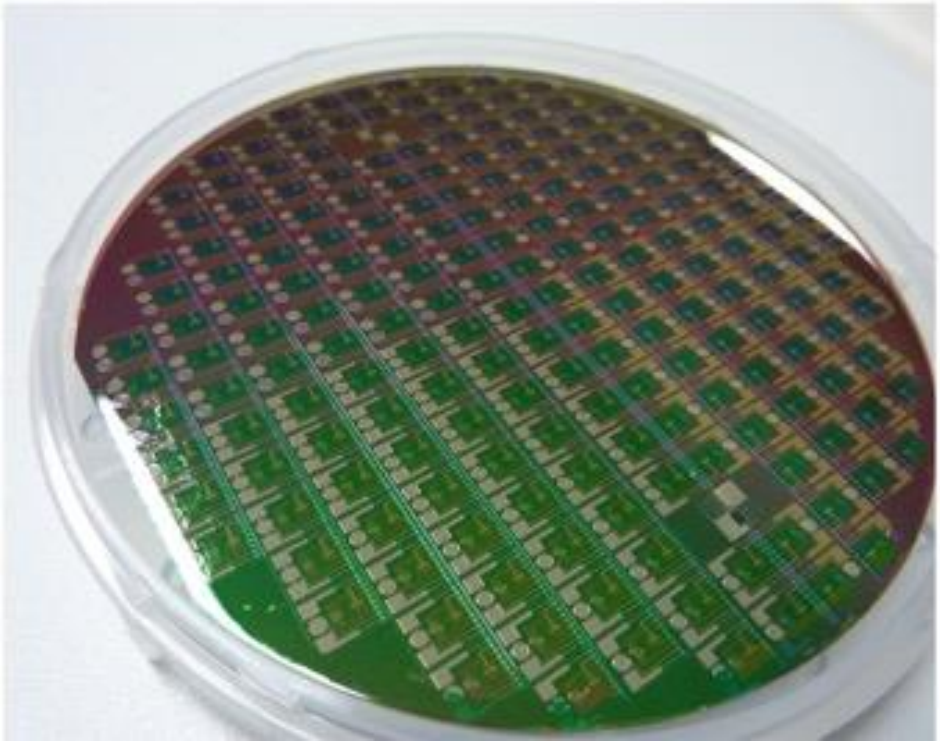

Figure 1: mass fabrication of SiO_2/Si_3N_4 pH-ChemFET chips using silicon-based technologies

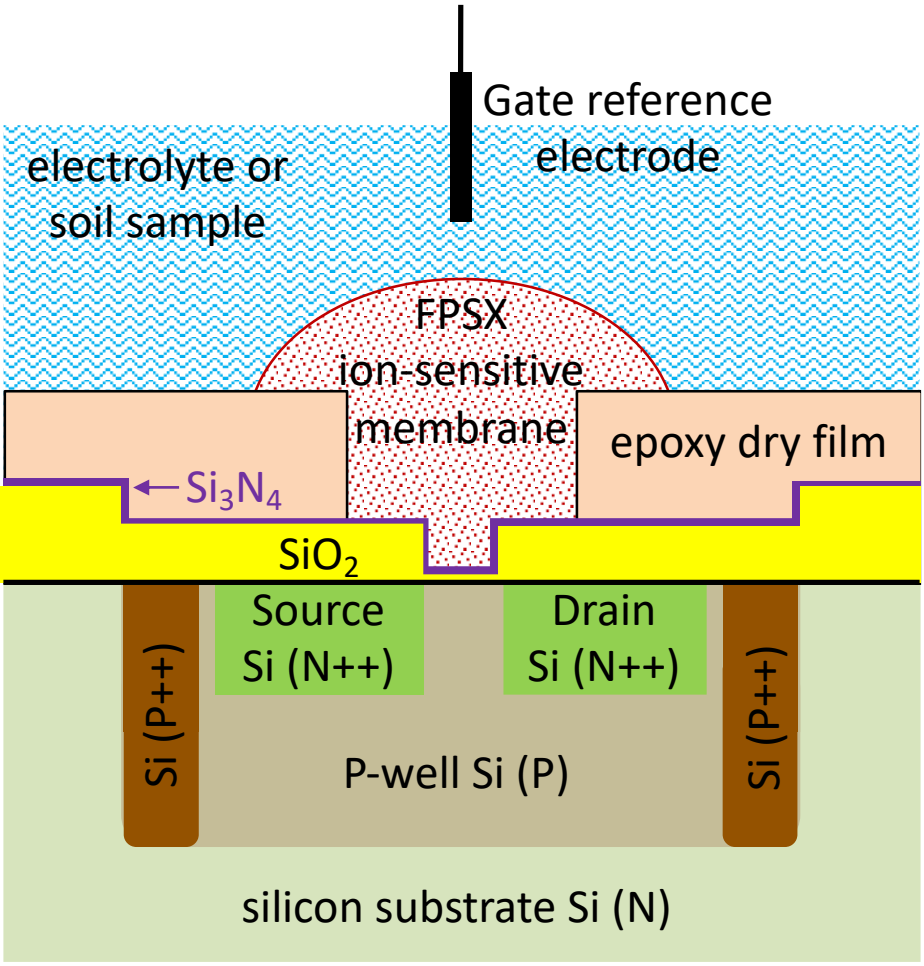

Figure 2: schematic cross section of the proposed ISFET device

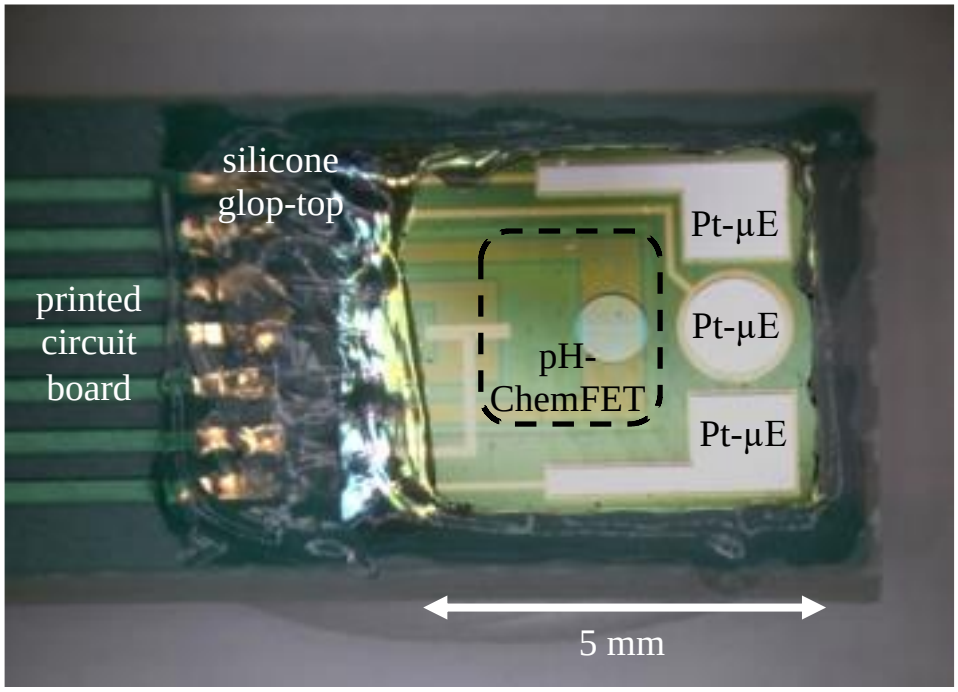

Figure 3: integration of pH-ChemFET silicon chips on printed circuit board

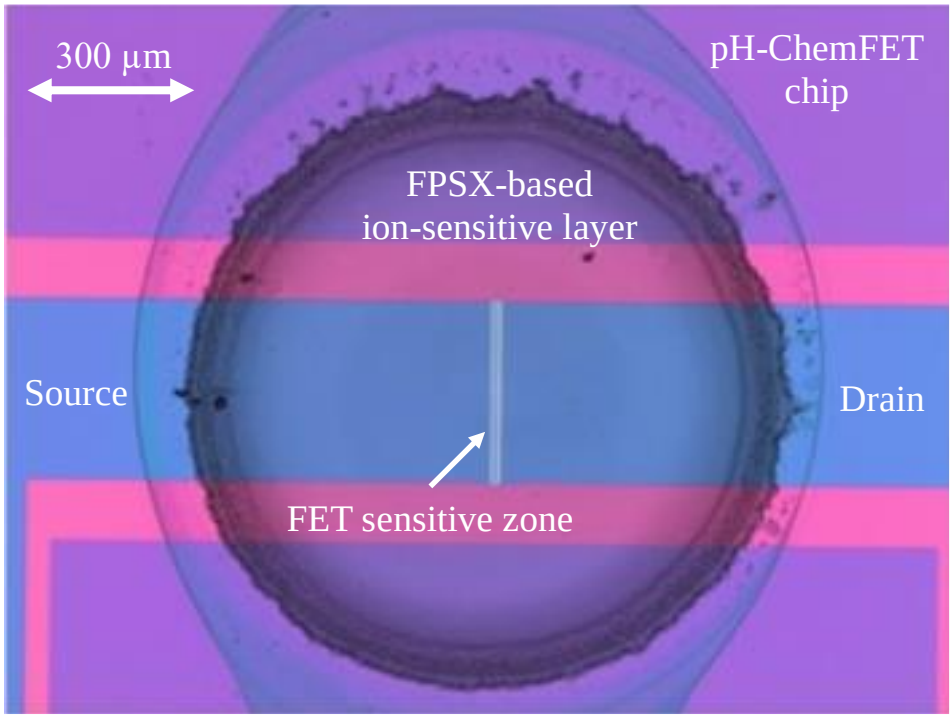

Figure 4: dip-coating deposition of the fluoropolysiloxane-based ion-sensitive layer on the SiO_2/Si_3N_4 pH-ChemFET sensitive zone

Figure 5: analysis of clay-silt soil matrices using ChemFET-based sensors

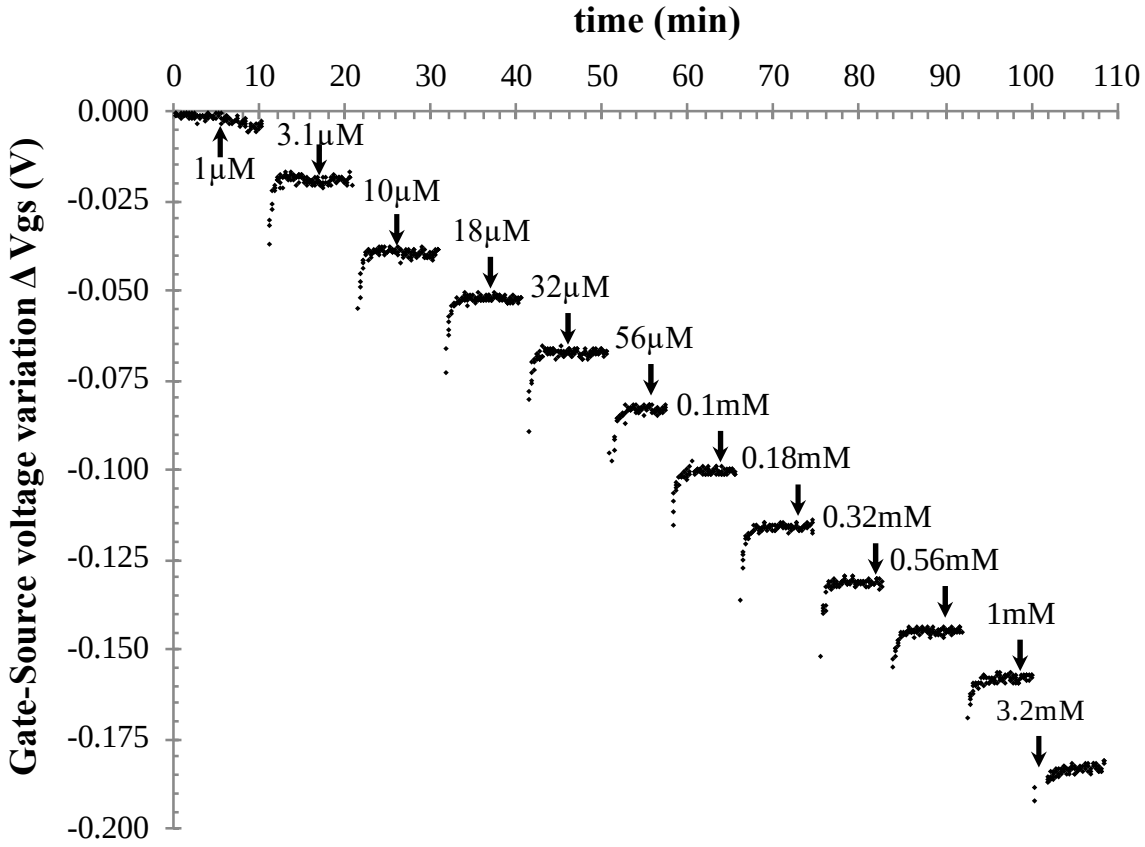

Figure 6: temporal variations of the pNH4-ISFET device with increasing [NH_4^+] concentration

(studied case: nonactine ionophore and KTpClBP ionic additive in a FPSX-based polymer matrix)

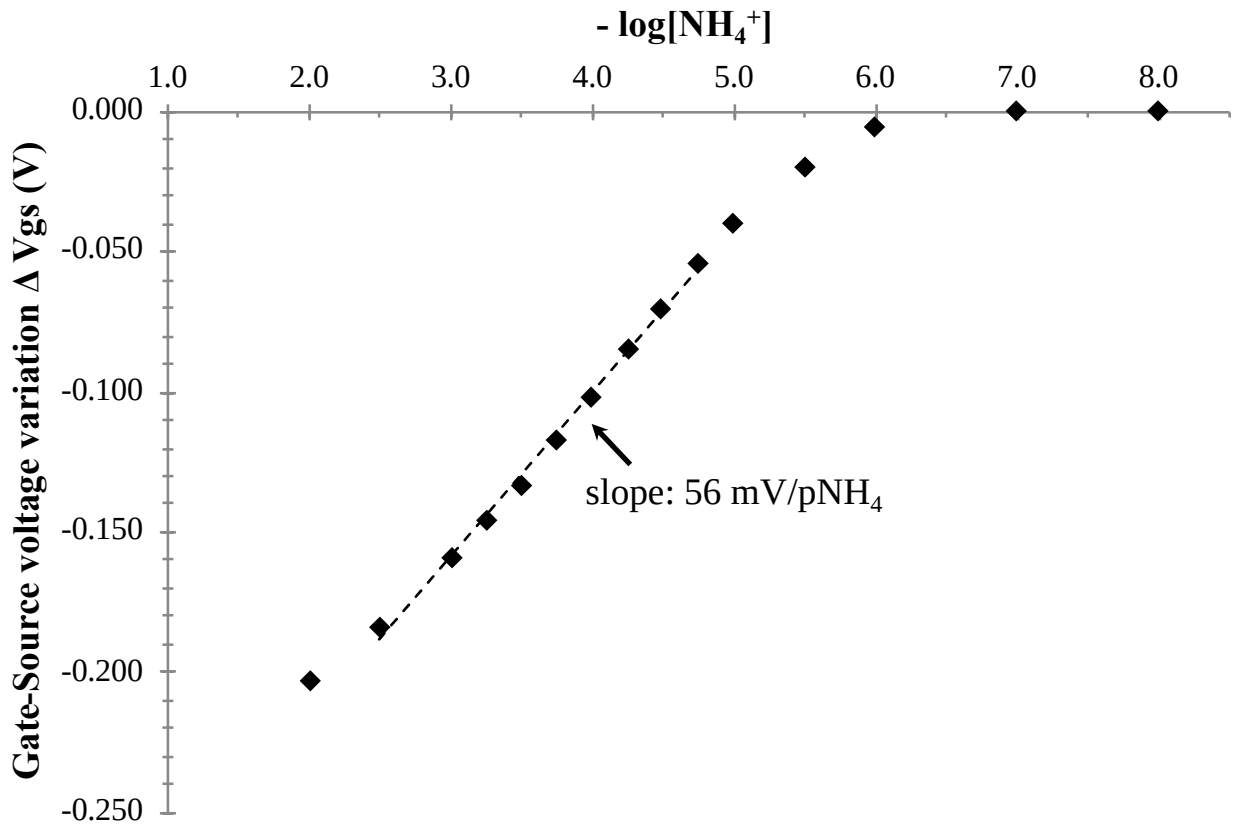

Figure 7: pNH_4-ISFET analytical response in NH_4NO_3 aqueous solutions using a calomel reference electrode (potentiometric measurement accuracy: ± 2.5 mV, studied case: nonactine ionophore and KTpClBP ionic additive in a FPSX-based polymer matrix)

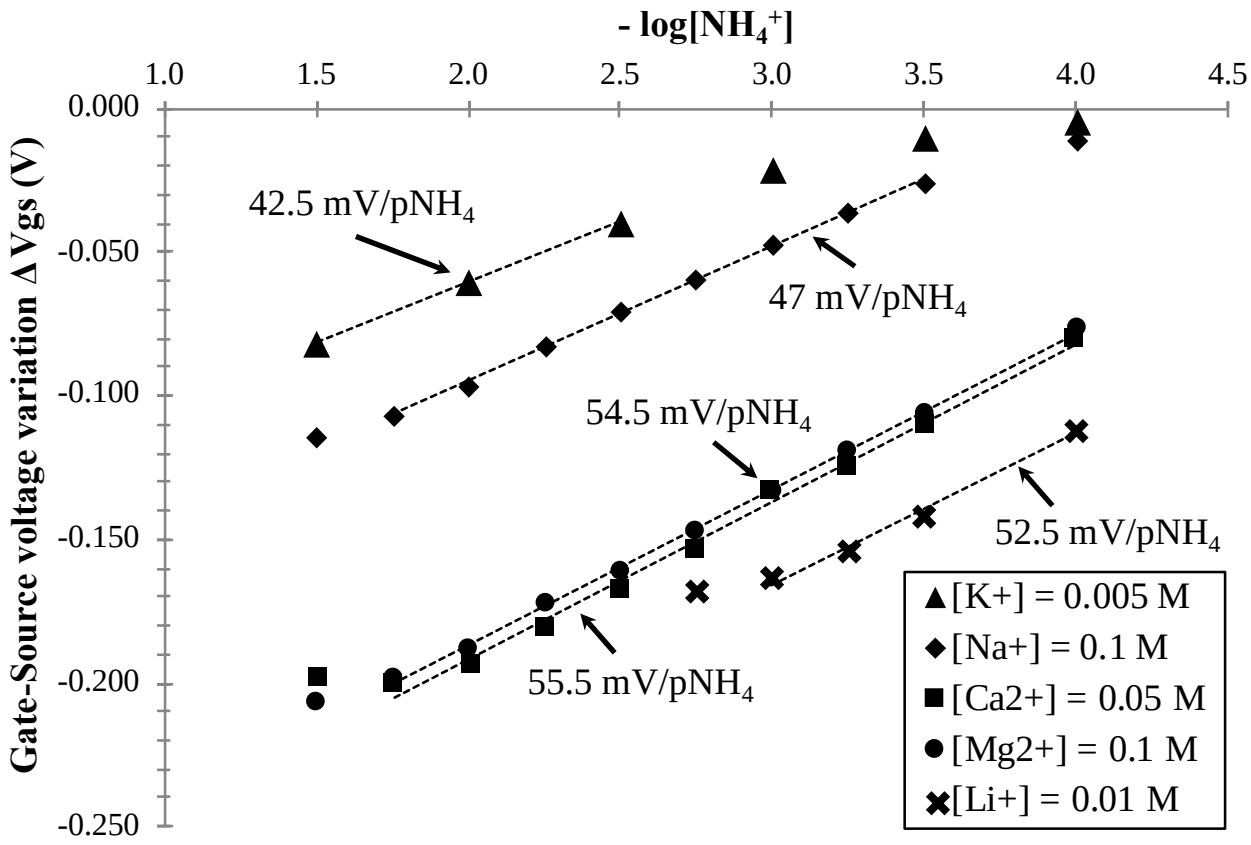

Figure 8: pNH_4-ISFET analytical response in presence of various interfering ions (FIM method) using a calomel reference electrode (potentiometric measurement accuracy: ± 2.5 mV, studied case: nonactine ionophore and KTpClBP ionic additive in a FPSX-based polymer matrix)

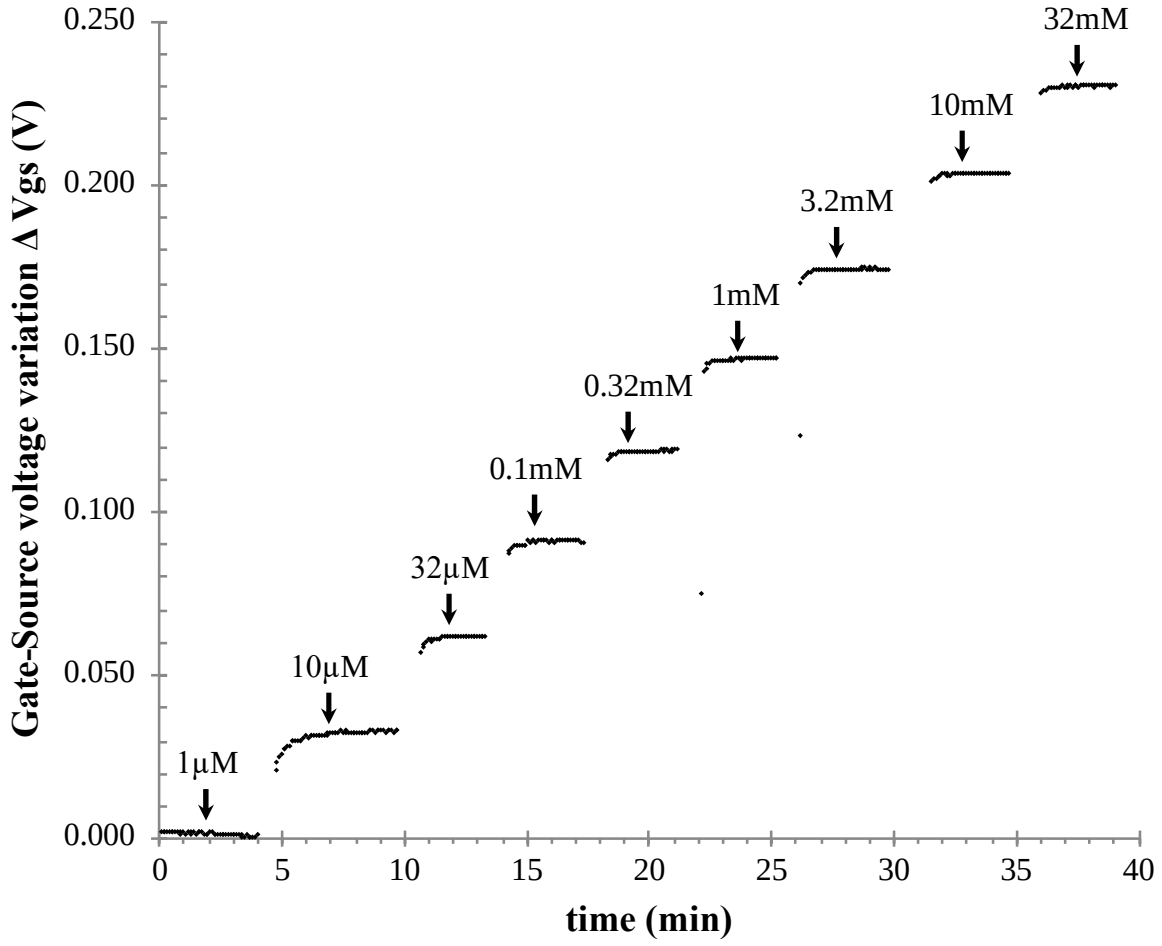

Figure 9: temporal variations of the pNO_3-ISFET device with increasing [NO_3^-] concentration (studied case: TDDAN ionophore and KTFBP ionic additive in a FPSX-based polymer matrix)

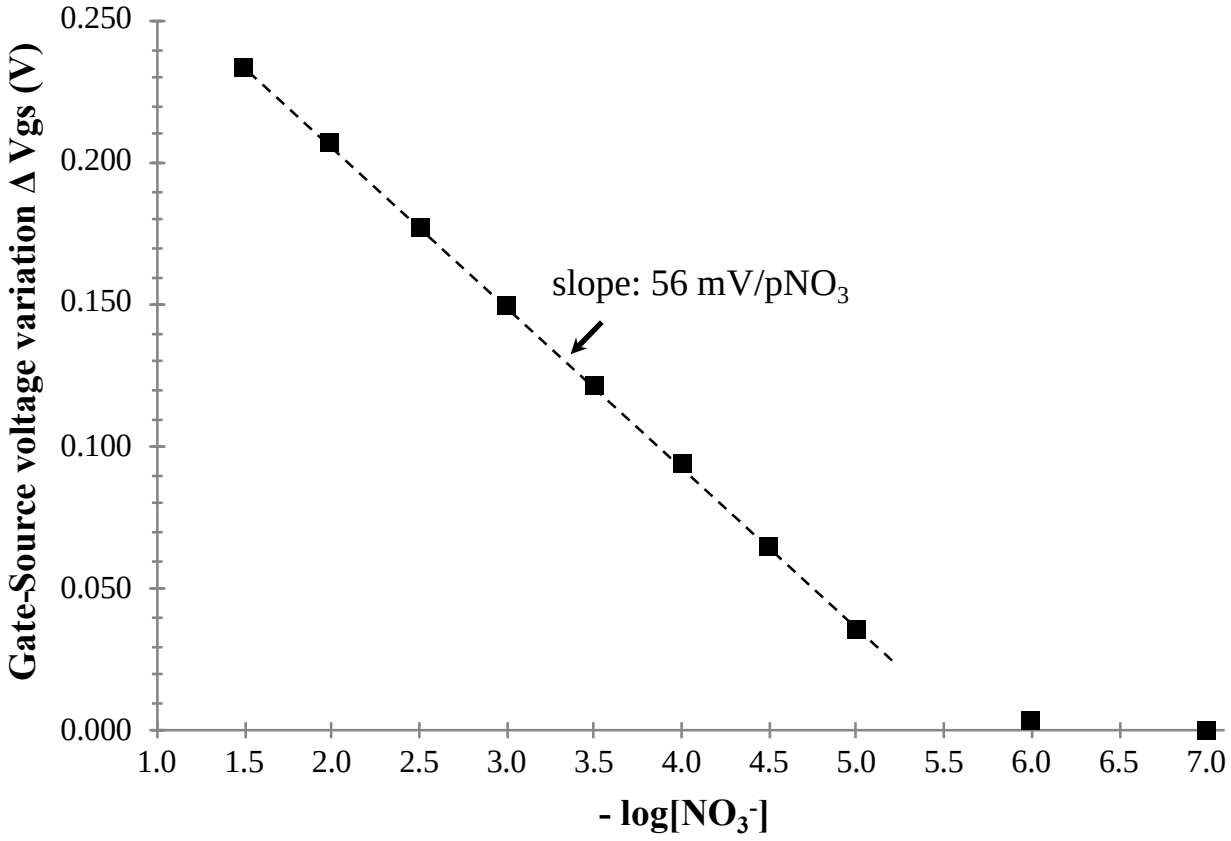

Figure 10: pNO_3-ISFET analytical response in NH_4NO_3-based aqueous solutions using a calomel reference electrode (potentiometric measurement accuracy: ± 1 mV, (studied case: TDDAN ionophore and KTFBP ionic additive in a FPSX-based polymer matrix)

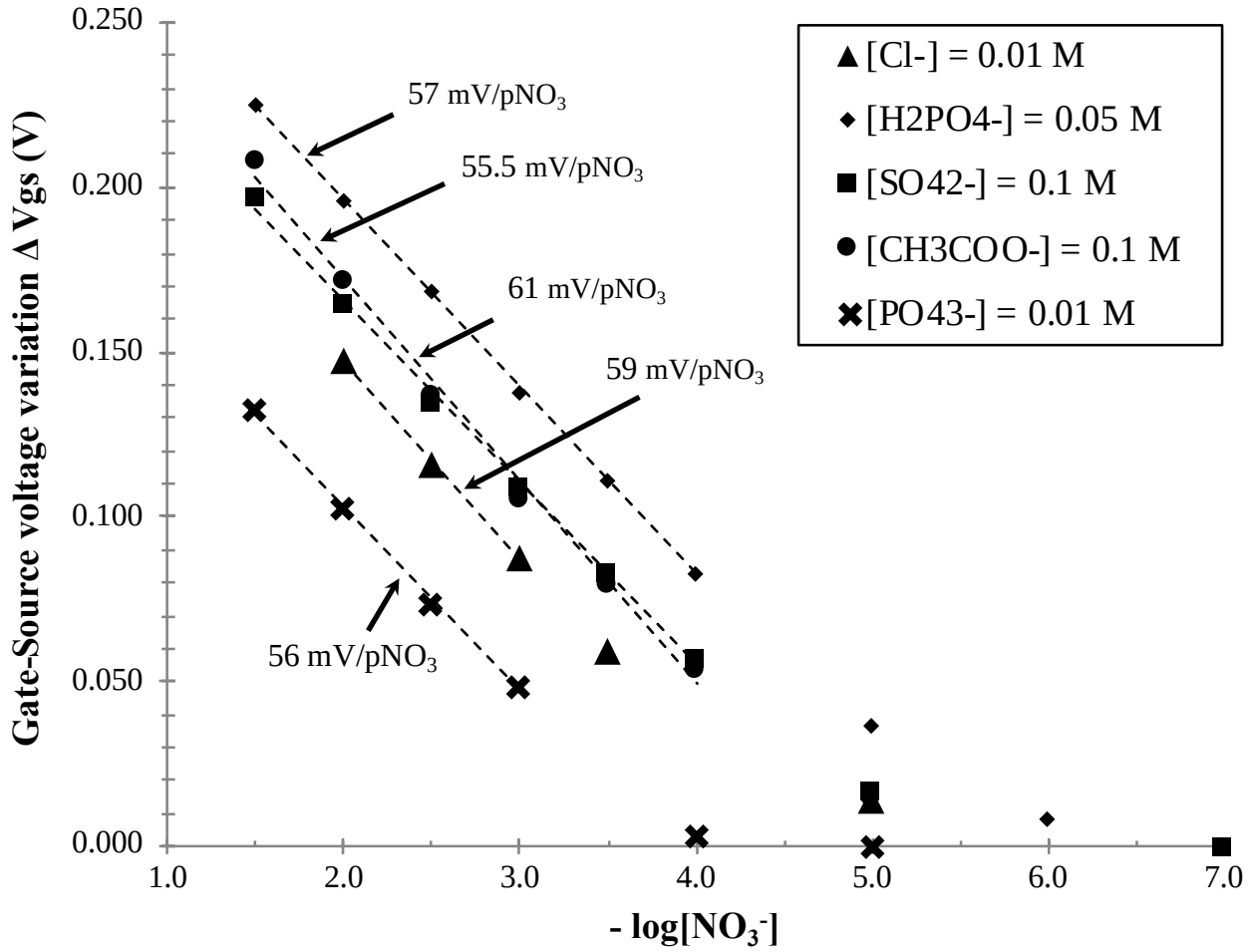

Figure 11: pNO_3-ISFET analytical response in presence of various interfering ions (FIM method) using a calomel reference electrode (potentiometric measurement accuracy: ± 1 mV, (studied case: TDDAN ionophore and KTFBP ionic additive in a FPSX-based polymer matrix)

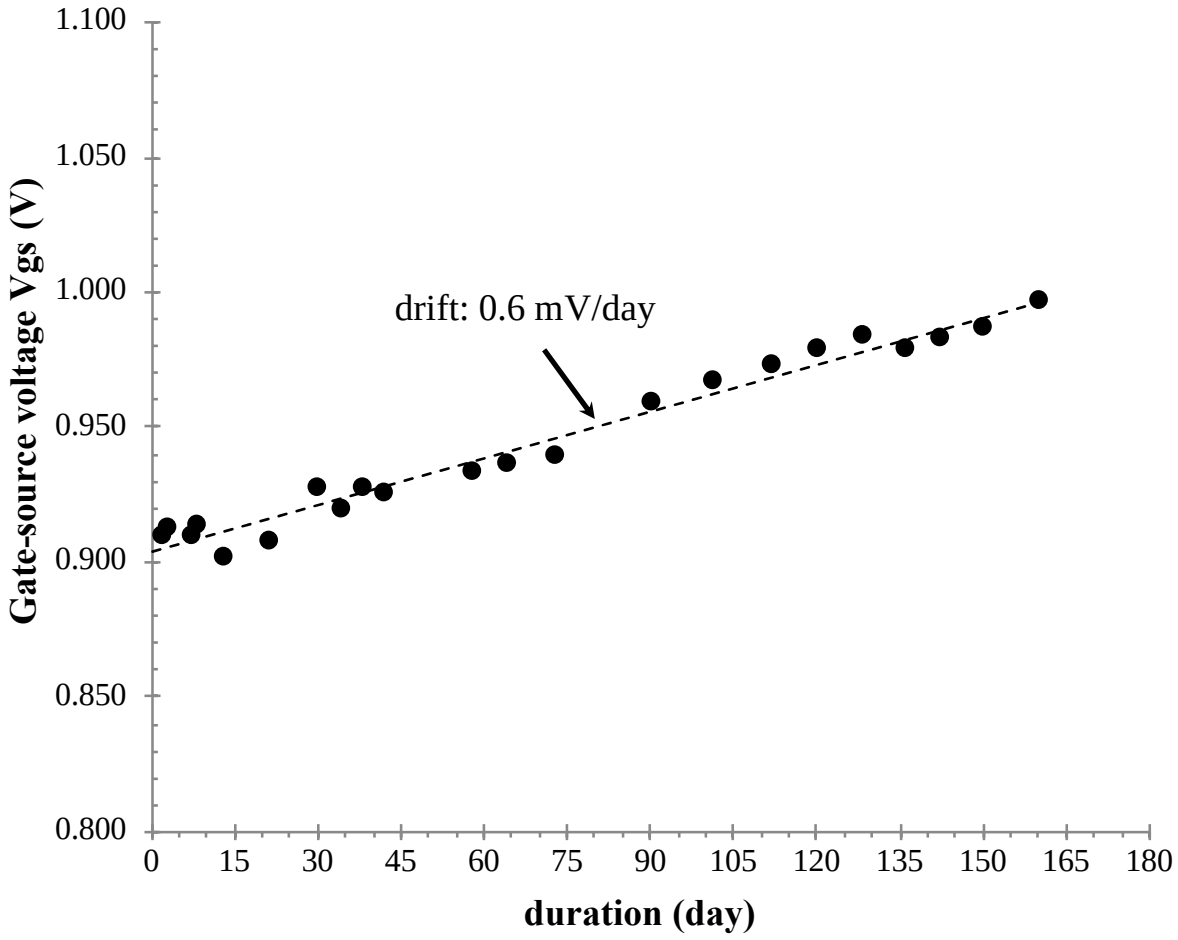

Figure 12: temporal drift of a pH-ISFET sensor buried into an acidic (pH = 4.7) clay-silt soil matrix for a six-month period (potentiometric measurement accuracy: ± 1 mV)

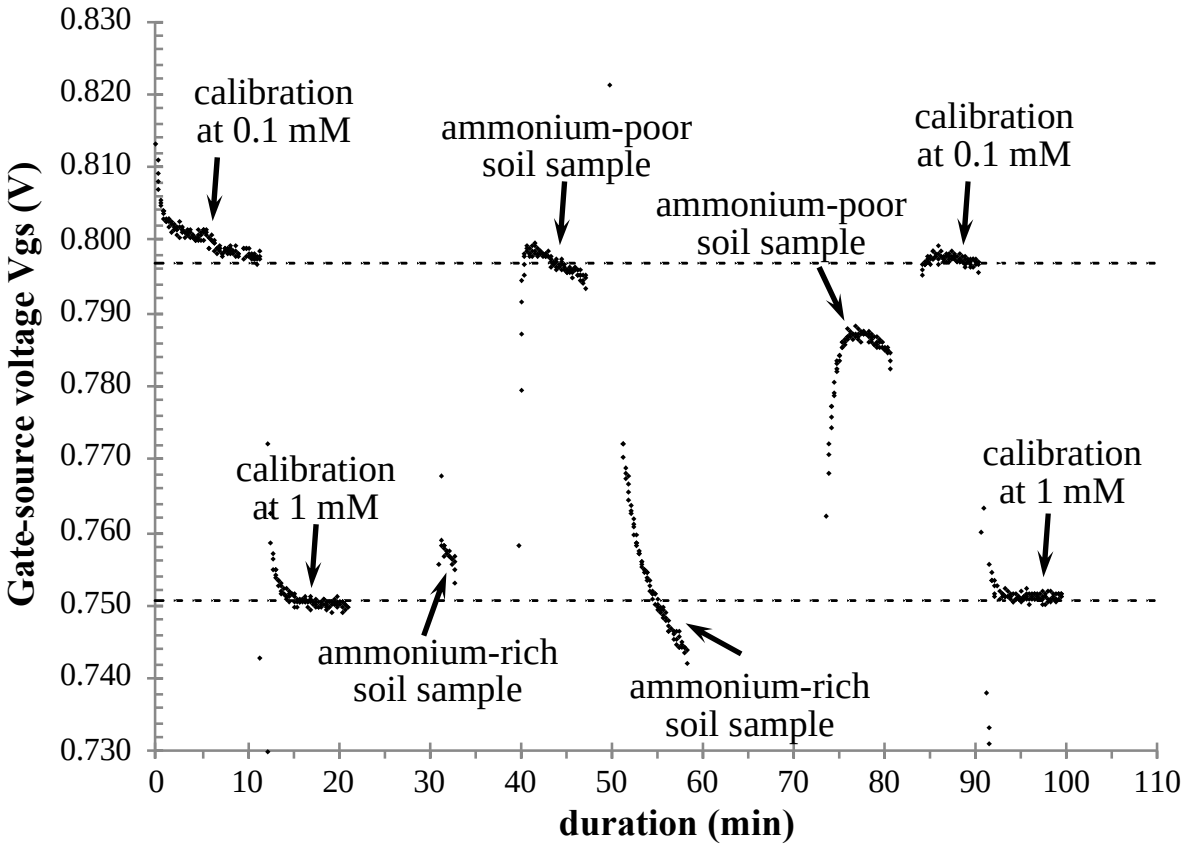

Figure 13: monitoring of the pNH4-ISFET response according to the following routine: calibration into NH_4NO_3 solutions (10^{-4} and 10^{-3} M), burying into NH_4^+-rich and NH_4^+-poor soil pots, final calibration into NH_4NO_3 solutions (10^{-4} and 10^{-3} M)